

**FABRICATION OF 3D DOUBLE-NETWORK
CNC/ALG/PEGDA PRINTED CONSTRUCTS
SEEDED WITH C2C12 MYOBLASTS FOR
BIOPRINTING APPLICATIONS**

ANUSHA WEI A/P ASOHAN

UNIVERSITI SAINS MALAYSIA

2023

**FABRICATION OF 3D DOUBLE-NETWORK
CNC/ALG/PEGDA PRINTED CONSTRUCTS
SEEDED WITH C2C12 MYOBLASTS FOR
BIOPRINTING APPLICATIONS**

by

ANUSHA WEI A/P ASOHAN

**Thesis submitted in fulfilment of the requirements
for the degree of
Master of Science**

September 2023

ACKNOWLEDGEMENT

I would like to give thanks to God for His grace in seeing me through the completion of this project. To my parents and brother, I am deeply grateful for your love and prayers, for your continuous support and encouragement that made it possible for me to come this far. I am truly thankful to my family and friends for lending an ear, for offering a kind word, thank you for making this experience a wonderful one.

I would also like to express my heartfelt gratitude to my supervisor, Dr Yazmin Bustami, for the opportunity to undertake this interesting project. This field has opened my eyes to the many possibilities research and science has to offer. It has been a great experience learning from her and sharing the excitement and passion of this project. I am very thankful for her guidance and support throughout this journey.

I would like to extend my deep gratitude to Dr Adelina and the staff in Malaysian Institute of Pharmaceuticals and Nutraceuticals (iPharm) where I worked part of my research at. I am very thankful to Dr Adel for guiding me during my cell culture training, for sharing her knowledge and expertise with me.

I wish to thank the staff and postgraduate students from the School of Industrial Technology, USM for their warm welcome and for allowing me to work part of my research in their laboratory. I would also like to thank the laboratory technicians and staff from the School of Biological Sciences, for assisting me and helping me in many ways throughout my project.

I wish to also extend my deep appreciation to my senior, Nurshafiqah Jasme who has guided me and offered me many valuable advice and suggestions during my project. I am truly grateful for all the knowledge and experience she has shared with me.

TABLE OF CONTENTS

ACKNOWLEDGEMENT	ii
TABLE OF CONTENTS	iii
LIST OF TABLES	vii
LIST OF FIGURES	viii
LIST OF SYMBOLS	xi
LIST OF ABBREVIATIONS	xii
LIST OF APPENDICES	xiii
ABSTRAK	xiv
ABSTRACT	xvi
CHAPTER 1 INTRODUCTION	1
1.1 Research Background.....	1
1.2 Problem Statement	2
1.3 Hypothesis	3
1.4 Objectives.....	4
CHAPTER 2 LITERATURE REVIEW	5
2.1 Introduction to 3D bioprinting	5
2.2 3D Bioprinting Techniques	6
2.3 Hydrogel-based bioink for bioprinting applicatioins	9
2.3.1 Alginate	9
2.3.2 Cellulose Nanocrystals (CNCs) as a reinforcing agent.....	11
2.3.3 Poly(ethylene glycol) diacrylate (PEGDA)	13
2.3.4 Double network hydrogel.....	14
2.4 Requirements of a bioink	15
2.4.1 Mechanical Properties	16
2.4.2 Printability.....	17

2.4.3	Biocompatibility.....	17
2.4.4	Shape and structure	18
CHAPTER 3 MATERIALS AND METHODOLOGY		21
3.1	Materials.....	21
3.2	Methods.....	22
3.2.1	Isolation and Extraction of Cellulose Nanocrystals	22
3.2.2	Characterisation of the extracted CNC using Transmission Electron Microscopy (TEM).....	23
3.2.3	Preparation of CNC/Alg/PEGDA hydrogel.....	23
3.2.3(a)	Alg solution	24
3.2.3(b)	CNC solution	24
3.2.3(c)	PEGDA solution	24
3.2.3(d)	Irgacure 2959 solution.....	24
3.2.3(e)	Calcium sulphate solution.....	24
3.2.4	Formulation of CNC/Alg/PEGDA hydrogel.....	24
3.2.4(a)	Preparation of CNC/Alg/PEGDA hydrogel.....	25
3.2.4(b)	Rheological Analysis of CNC/Alg/PEGDA Formulations	26
3.2.4(c)	Compression Tests of Mechanical Properties of CNC/Alg/PEGDA hydrogel construct.....	27
3.2.4(d)	Observation of CNC/Alg/PEGDA hydrogel constructs swelling behaviour.....	27
3.2.4(e)	Observation of the morphology of CNC/Alg/PEGDA hydrogel constructs	28
3.2.5	Culturing C2C12 myoblast cell line.....	29
3.2.5(a)	Preparation of complete medium.....	29
3.2.5(b)	Thawing C2C12 myoblasts.....	29
3.2.5(c)	Proliferation of C2C12 myoblasts	30
3.2.5(d)	Cell passaging of C2C12 myoblasts	30

3.2.6	3D Bioprinting of CNC/Alg/PEGDA hydrogel formulation	31
3.2.7	Preparation of CNC/Alg/PEGDA cell-laden bioink	32
3.2.7(a)	Fabrication of 3D-bioprinted cell-laden constructs	32
3.2.8	Analysis of cell viability within the printed construct	33
3.2.9	Analysis of printed construct using Field Emission Scanning Electron Microscopy (FE SEM).....	34
CHAPTER 4 RESULTS.....		36
4.1	Production and Morphology of Cellulose Nanocrystals (CNCs).....	36
4.2	Formulation of CNC/Alg/PEGDA hydrogels	38
4.3	Rheological Properties of CNC/Alg/PEGDA hydrogel formulations.....	39
4.3.1	Determination of shear thinning property	39
4.3.2	Determination of storage and loss moduli	41
4.4	Determination of mechanical properties of CNC/Alg/PEGDA hydrogel construct	43
4.4.1	Physical characteristics of CNC/Alg/PEGDA hydrogel construct	43
4.4.2	Swelling Properties of CNC/Alg/PEGDA hydrogel constructs.....	46
4.4.3	Compression test of CNC/Alg/PEGDA hydrogel construct	48
4.5	Morphology of CNC/Alg/PEGDA 3D Manual Constructs.....	49
4.6	3D Bioprinting process of CNC/Alg/PEGDA bioink	50
4.7	Cell Viability of CNC/Alg/PEGDA cell-laden bioink.....	52
4.8	Morphology and porosity of bioprinted CNC/Alg/PEGDA construct.....	58
CHAPTER 5 DISCUSSION		60
5.1	Production and Morphology of Cellulose Nanocrystals	60
5.2	Formulation of CNC/Alg/PEGDA hydrogel.....	61
5.3	Bioprinting of CNC/Alg/PEGDA bioink	68
CHAPTER 6 CONCLUSION AND FUTURE RECOMMENDATIONS.....		78
6.1	Conclusion.....	78

6.2	Recommendations for Future Research	79
	REFERENCES.....	81
	APPENDICES	
	LIST OF PUBLICATIONS	

LIST OF TABLES

	Page
Table 3.1	List of materials used and respective manufacturer.21
Table 3.2	Nine formulations of CNC/Alg/PEGDA with different concentrations.25
Table 3.3	Bioprinter settings for extrusion-based bioprinting.31
Table 4.1	Power-law index (n) and consistency index (K) of the different CNC/Alg/PEGDA bioinks.39
Table 4.2	Formulation of CNC/Alg/PEGDA bioinks with different concentrations.44
Table 4.3	Comparison of water content and swelling ratio of native articular cartilage with CNC/Alg/PEGDA hydrogel construct at different formulations. The water content for the formulations of high Alg concentration (4%) are within the range of 79% to 84% while the formulations with low Alg concentration (1% and 2.5%) had more than 85%. Three replicates are used for each formulation. bioinks ...48
Table 4.4	3D printed constructs of different heights after UV photocrosslinking.51

LIST OF FIGURES

	Page
Figure 2.1	Schematic diagram of three main types of bioprinting techniques namely (A) Laser-assisted Bioprinting, (B) Inkjet Bioprinting and (C) Microextrusion Bioprinting. Adapted from McGivern et al., (2021) 8
Figure 2.2	Schematic representation of ionic crosslink interaction between alginate and calcium ions forming an egg-box structure. Adapted from Abasalizadeh et al., (2020). 10
Figure 2.3	Schematic representation of the photopolymerization process of PEGDA and a photoinitiator I2959. 14
Figure 3.1	Schematic illustration of the manual extrusion process of CNC/Alg/PEGDA formulations. The important process includes A: soft gel formulation preparation, B: extrusion of hydrogel into a glass mould and C: construct treated with UV irradiation at 365 nm post extrusion. 26
Figure 3.2	Schematic illustration of bioprinting of CNC/Alg/PEGDA bioink using extrusion based bioprinter. The important process includes A: mixing of cell suspension into CNC/Alg/PEGDA bioink, B: fabrication of 3D construct using a 3D bioprinter, C: exposure of printed construct to UV irradiation, D: incubation of CNC/Alg/PEGDA constructs at 37°C in 5% CO ₂ 33
Figure 4.1	TEM image of CNC extracted from OPT after acid hydrolysis treatment with magnification of A: 20 000X and B: 40 000X. The CNC exhibit typical rod-like structure with an average diameter of around 7 ± 2.4 nm and average length of around 113 ± 20.7 nm. 37
Figure 4.2	The CNC/Alg/PEGDA formulation showed A: liquid-like mixture before the addition of CaSO ₄ , and B: soft-gel mixture after the addition of CaSO ₄ 38

Figure 4.3	Flow curves of four different CNC/Alg/PEGDA hydrogel formulations; (●) F4 :[4%CNC:1%Alg:40%PEGDA]; (▲) F2 :[4%CNC:1%Alg:10%PEGDA]; (●) F3 :[1%Alg:40%PEGDA]; (▲) F1 :[1%Alg:10%PEGDA]. Data points represent actual data, and lines are power-law model fits. F2 and F4 hydrogel formulations show high shear thinning behaviour.	40
Figure 4.4	Flow curves of five different CNC/Alg/PEGDA hydrogel formulations; (■) F7 :[4%Alg:40%PEGDA; (■) F8 :[4%CNC:4%Alg:40%PEGDA]; (◆) F6 :[4%CNC:4%Alg:10%PEGDA]; (◆) F9 :[2%CNC:2.5%Alg:25%PEGDA]; (●) F5 :[4%Alg:10%PEGDA]. Data points represent actual data, and lines are power-law model fits. F6, F7, F8, and F9 hydrogel formulations high shear thinning behaviour.	40
Figure 4.5	Storage modulus, G' (square symbols) and loss modulus, G'' (triangle symbols) of four hydrogel formulations; F6: [4%CNC: 4%Alg: 10%PEGDA]; F8: [4%CNC: 4%Alg: 40%PEGDA]; F9: [2%CNC :2.5%Alg :25%PEGDA]; F7: [4%Alg: 40%PEGDA]. The storage modulus (G') was higher than the loss modulus (G'') for all the hydrogel formulations across the frequencies tested.	42
Figure 4.6	Observation of the swelling behaviour of F8 hydrogel construct with 4% CNC, 4% Alg and 40% PEGDA concentration at A: 0 hr of immersion and B: 48 hrs of immersion in PBS solution, pH 7.4. The hydrogel construct remained stable throughout the course of 48 hrs.	47
Figure 4.7	Observation of the compression behaviour of UV crosslinked hydrogel construct A: without CNC [4% Alg: 40% PEGDA] and B: with CNC [4% CNC: 4% Alg: 40% PEGDA] after manual compression.	49

Figure 4.8	SEM images of freeze-dried F8 [4% CNC: 4% Alg: 40% PEGDA] construct at magnification of A: 100x and B: 801x. The presence of CNCs are indicated with red arrows. The hydrogel contains pores with irregular oblong shapes.	50
Figure 4.9	The image of CNC/Alg/PEGDA bioprinted construct encapsulated with C2C12 myoblasts was viewed with inverted microscope under 40x magnification. The red arrows indicate the presence of CNC within the construct.	53
Figure 4.10	Inverted microscope image showing the attachment of C2C12 myoblasts to the CNC under 100x magnification. The red arrows indicate the attachment of cells to CNC.	54
Figure 4.11	Fluorescence microscope images showing live (green) C2C12 myoblasts encapsulated in the CNC/Alg/PEGDA bioink on day 1, 7 and 14 to 16.	55
Figure 4.12	Fluorescence microscope images showing dead (red) C2C12 myoblasts encapsulated in the CNC/Alg/PEGDA bioink on day 1, 7 and 14 to 16.	56
Figure 4.13	Cell viability of C2C12 myoblasts before embedding and after embedding in the CNC/Alg/PEGDA bioink on day 1, 7 and 14 to 16.	57
Figure 4.14	Average number of live (green) and dead (red) cells of C2C12 myoblasts encapsulated in the CNC/Alg/PEGDA bioink on day 1, 7 and 14 to 16. The average number of live cells remained almost the same while the dead cells decreased notably.	57
Figure 4.15	SEM images of CNC/Alg/PEGDA construct without cells at magnification of A: 1000x and B: 5000x.	59
Figure 4.16	SEM images of CNC/Alg/PEGDA construct seeded with C2C12 myoblasts at magnification of A: 4000x; B: 5000x. The red arrows indicate the attachment of the C2C12 myoblasts to the bioink.	59

LIST OF SYMBOLS

μL	Microliter
mL	Milliliter
w/v	Weight per volume
v/v	Volume per volume
nm	Nanometer
μm	Micrometer
mm	Millimeter
min	Minute
hr	Hour
g	Gram
$^{\circ}\text{C}$	Degree celcius
%	Percentage
x	Times
rpm	Revolutions per minute
H	Height

LIST OF ABBREVIATIONS

3D	Three-dimensional
Alg	Alginate
CAD	Computer Aided Design
CaSO ₄	Calcium sulphate
CNC	Cellulose Nanocrystal
dH ₂ O	Distilled water
DMEM	Dulbecco's Modified Eagle Medium
ECM	Extracellular matrix
FBS	Fetal Bovine Serum
FTIR	Fourier Transformed Infrared Spectroscopy
H ₂ SO ₄	Sulfuric acid
KOH	Potassium hydroxide
OPT	Oil Palm Trunk
PBS	Phosphate Buffer Saline
PEG	Poly(ethylene glycol)
PEGDA	Poly(ethylene glycol) diacrylate
RT	Room Temperature
SEM	Scanning Electron Microscope
UV	Ultraviolet
LVR	Linear Viscoelastic Region
TEM	Transmission Electron Microscope

LIST OF APPENDICES

Appendix A	Grinded OPT Fibres
Appendix B	Extractives of OPT fibres dewaxed using Soxhlet extraction
Appendix C	Delignification of OPT fibres via bleaching
Appendix D	Removal of hemicellulose region using KOH
Appendix E	Washing and rinsing step after acid hydrolysis
Appendix F	Dialysis of CNC samples
Appendix G	Grinded CNC samples after freeze drying
Appendix H	Oscillation amplitude sweep (0.1-100%) of F6: [4%CNC:4%Alg:10%PEGDA] hydrogel with a fixed frequency of 1 Hz.
Appendix I	Oscillation amplitude sweep (0.1-100%) of F7: [4%Alg:10%PEGDA] hydrogel with a fixed frequency of 1 Hz.
Appendix J	Oscillation amplitude sweep (0.1-100%) of F8: [4%CNC:4%Alg:40%PEGDA] hydrogel with a fixed frequency of 1 Hz.
Appendix L	Oscillation amplitude sweep (0.1-100%) of F9: [2%CNC:2.5%Alg:25%PEGDA] hydrogel with a fixed frequency of 1 Hz.
Appendix M	3D bioprinter set up in the biosafety cabinet
Appendix N	3D square block designed using Tinkercad for bioprinting

**FABRIKASI DWI-RANGKAIAN 3D CNC/ALG/PEGDA KONSTRUK
CETAKAN DISEMAI DENGAN MIOBLAS C2C12 UNTUK APLIKASI
PENCETAKAN BIO**

ABSTRAK

Pencetakan bio 3D menawarkan alternatif yang mengalakkan untuk perbaikan dan regenerasi rawan sendi menggunakan gerakan lapisan demi lapisan yang ditentukan oleh perisian bantuan komputer (CAD). Dalam projek ini, satu bio-ink untuk aplikasi biopencetakan telah dirumuskan menggunakan nanokristal selulosa (CNCs), alginat (Alg), dan poli(etilena glikol) diakrilat (PEGDA) menggunakan pendekatan rangka rangkap jaringan ganda di mana hidrogel terlebih dahulu dirangkap secara ionik dengan ion Ca^{2+} dan kemudiannya dirangkap secara foto di bawah sinaran UV pada 365nm selepas pengestrusan. Sifat reologi, perilaku pembengkakan dan sifat mekanikal formulasi dinilai untuk menentukan formulasi yang paling sesuai untuk biopencetakan. Kemudian, kebolehcapaian pencetakan formulasi CNC/Alg/PEGDA yang dipilih dinilai menggunakan biopencetakan berasaskan ekstrusi. Seterusnya, biokompatibiliti untuk formulasi CNC/Alg/PEGDA yang terpilih ditentukan menggunakan mioblas C2C12. Sel tersebut disemai ke dalam hidrogel, diikuti oleh proses biopencetakan. Peratusan kehidupan sel telah dinilai menggunakan asai 'Live/Dead' selama tempoh 14-16 hari. Struktur dalaman dan keporosan konstruk biopencetakan dengan dan tanpa sel dianalisis menggunakan mikroskopi pengimbasan elektron (SEM). Berdasarkan hasil awalan, Formulasi 8 (F8) dengan kepekatan 4% CNC, 4% Alg, dan 40% PEGDA menunjukkan tingkah laku pencairan dengan indeks hukum kuasa $\eta < 1$ dan modulus penyimpanan yang dominan berbanding modulus kehilangan ($G' > G''$), data ini menunjukkan kebolehcapaian pencetakan yang baik dan

kekemasan bentuk. Selain itu, kandungan air (79.5%) ditemui hampir sama dengan rawan sendi semula jadi. Konstruk F8 juga menunjukkan sifat mekanikal yang baik dan struktur yang kukuh dan fleksibel ketika dikenakan beban. Apabila diaplikasikan menggunakan pencetak 3D, konstruk yang dicetak menunjukkan kebolehan penumpukan yang baik dan dapat mengekalkan ketinggian mereka. Walau bagaimanapun, dengan peningkatan ketinggian konstruk, dimensi dan bentuk ditemui berbeza dari reka bentuk asal disebabkan oleh penyebaran hidrogel. Menariknya, mioblas C2C12 dalam konstruk biopencetakan menunjukkan kebolehvitalan sel sebanyak 53%, 77%, dan 94% selepas 1, 7, dan 14 hingga 16 hari inkubasi, masing-masing. Walau bagaimanapun, bilangan sel yang boleh hidup kekal hampir sama dan tiada proliferasi yang signifikan diperhatikan. Analisis SEM menunjukkan struktur liang yang sangat berpori dan mikroliang teragih sekata antara $2.546 \pm 0.7217 \mu\text{m}$ hingga $12.06 \pm 2.034 \mu\text{m}$. Secara keseluruhan, CNC memainkan peranan penting dalam pelekatan sel dalam konstruk biopencetakan. Bio-ink yang dirumuskan menunjukkan potensi yang menjanjikan dalam aplikasi biopencetakan 3D.

**FABRICATION OF 3D DOUBLE-NETWORK CNC/ALG/PEGDA
PRINTED CONSTRUCTS SEEDED WITH C2C12 MYOBLASTS FOR
BIOPRINTING APPLICATIONS**

ABSTRACT

3D bioprinting offers a promising alternative for articular cartilage repair and regeneration using a layer-by-layer predetermined movement from a computer aided (CAD) software. In this project, a bioink for bioprinting applications was formulated using cellulose nanocrystals (CNCs), alginate (Alg), and poly(ethylene glycol) diacrylate (PEGDA). Firstly, different formulations of CNC/Alg/PEGDA were formulated using a double network crosslinking approach where the hydrogel was first ionically crosslinked with Ca^{2+} ions and subsequently photo-crosslinked under UV irradiation at 365nm post-extrusion. The rheological properties, swelling behaviour, and mechanical properties of the formulations were assessed to determine the optimal formulation for bioprinting. Then, the printability of the selected CNC/Alg/PEGDA formulation was evaluated using an extrusion based bioprinter. Next, the biocompatibility of the selected CNC/Alg/PEGDA formulation was determined using C2C12 myoblasts. The cells were seeded into the hydrogel, followed by the bioprinting process. The viability of cells was assessed using Live/Dead assay for a period of 14 to 16 days. The internal structure and porosity of the bioprinted construct with and without cells was analysed using scanning electron microscopy (SEM). Based on the preliminary results, Formulation 8 (F8) with the concentration of 4% CNC, 4% Alg and 40% PEGDA demonstrated shear-thinning behaviour with power-law index $\eta < 1$ and storage modulus dominance over loss modulus ($G' > G''$), indicating good printability and shape fidelity. In addition, the water content (79.5%) is almost similar

to the native articular cartilage. The F8 construct also displayed good mechanical properties and demonstrated a tough and flexible structure when under load. When applied using a 3D bioprinter, the printed constructs showed good stacking ability and were able to retain their heights. However, as the construct height increased, the dimensions and shape deviated from the original design due to the hydrogel spreading. Interestingly, the C2C12 myoblasts in the bioprinted construct exhibited a cell viability of 53%, 77%, and 94% after 1, 7 and 14 to 16 days of incubation, respectively. However, the number of viable cells remained almost the same and no significant proliferation was observed. The SEM analysis revealed a highly porous and evenly distributed pore structure ranging from $2.546 \pm 0.7217 \mu\text{m}$ to $12.06 \pm 2.034 \mu\text{m}$. Overall, CNC played an important role in the attachment of cells within the bioprinted construct and the formulated bioink showed promising potential in 3D bioprinting applications.

CHAPTER 1

INTRODUCTION

1.1 Research Background

Tissue engineering is a rapidly evolving discipline that shows promising prospect in the restoration and regeneration of the damaged tissue and organs (Rider et al., 2018). The articular cartilage for instance is a highly valuable area of interest in this research field due to its compositional structure. While the human body is capable of self-healing, some parts of the body; like the articular cartilage, have limited capacity to repair themselves. The articular cartilage is a specialised connective tissue that provides low friction, lubricated and load-bearing surface for efficient joint movement (Fox et al., 2009). Once the articular cartilage is damaged, whether due to overuse, trauma or degenerative diseases, it can result in progressive impairment to the joint structure leading to joint pain and chronic disability (Cui et al., 2012; Medvedeva et al., 2018). Research on tissue-engineered articular cartilage has led to many promising tissue constructs *in vitro*, however, functionally equivalent engineered articular cartilage constructs and formation of phenotypically stable mature chondrocytes remain elusive and are often hampered by a limited control over the construct structure and mechanical and biological complexities (Medvedeva et al., 2018; Zylińska et al., 2018).

Three-dimensional (3D) bioprinting has emerged as a novel approach in addressing the limitations of cartilage repair and has recently been applied in the fabrication of tissue engineered cartilage (McGivern et al., 2021). In general, 3D bioprinting is an additive manufacturing process that dispenses bioink in a layer-by-layer manner to fabricate 3D constructs (Tan et al., 2021). One of the main components for successful bioprinting is the presence of a suitable bioink. The bioink

consists of a selection of suitable biomaterials and living cells that can promote tissue regeneration (Morgan et al., 2020). The selection of an ideal bioink is important in order to maintain the articular cartilage tissue's organised architecture. There are two main groups of hydrogel-based biomaterials: naturally derived and synthetically derived hydrogels which are usually used in bioink formulations. An ideal bioink should satisfy certain requirements, such as good mechanical properties, printability, biocompatibility, and shape and structure (Gu et al., 2020; Wang et al., 2015). Therefore, the challenge lies in formulating a bioink that meets all these requirements. For instance, bioinks used in cartilage bioprinting, the bioink needs to be tough and load bearing while also having elastic tendencies (Xu et al., 2013).

In this project, three different biomaterials namely alginate (Alg), poly(ethylene glycol) diacrylate (PEGDA), and cellulose nanocrystals (CNCs) were used to formulate the bioink. The combination of both natural (Alg and CNC) and synthetic polymers (PEGDA) gives rise to a double network (DN) hydrogel that enhances the mechanical properties and stability of the construct. The double network mechanism is achieved by the divalent ionic crosslinking with Ca^{2+} and photocrosslinking reaction with UV. The properties of the formulated CNC/Alg/PEGDA bioink were studied to initially assess its suitability and potential as an ideal bioink for 3D bioprinting applications.

1.2 Problem Statement

The most important component of bioprinting is the biomaterial selected. In this study, a biomaterial that is load bearing, mechanically stable and yet supports cell viability is essential to fulfill the characteristics required for articular cartilage bioprinting. Hydrogels are the gold standard biomaterials due to their ability to

mimic the microenvironment of the native tissue. They can be divided into two categories; naturally derived and synthetically derived hydrogels. However, past literatures have found it challenging to fabricate an ideal bioink using only natural or synthetic hydrogels individually. This is because naturally derived hydrogels tend to be mechanically weaker and do not offer long term stability. On the other hand, synthetically derived hydrogels lack the bioactivity and biological cues required to support cell viability and proliferation. Recently, there have been studies that look into the combination of both also known as hybrid bioinks. In this study, the combination of both natural (Alginate) and synthetic (PEGDA) is formulated to address and complement the limitations of each category with the intention of formulating a bioink that satisfies the requirements of an ideal bioink. Furthermore, the addition of cellulose nanocrystals (CNC) to the hybrid bioink is intended to function as a rheological modifier that supports the mechanical properties and biocompatibility of the hydrogel.

1.3 Hypothesis

The combination of both natural and synthetic polymers will produce a construct of high structural integrity without compromising the cell viability. The introduction of a double network hydrogel involving two crosslinking mechanisms will improve the mechanical stability of the construct during printing and post printing. The incorporation of cellulose nanocrystals in the bioink will also improve the flexibility and cell attachment of the bioink.

1.4 Objectives

1. To produce cellulose nanocrystals (CNC) from raw oil palm trunk (OPT) and fabricate a novel composite formulation using CNC/Alg/PEGDA.
2. To evaluate the rheological and mechanical properties of the double network CNC/Alg/PEGDA hydrogel and its printability using an extrusion based bioprinter.
3. To evaluate the cell viability of C2C12 myoblasts in the CNC/Alg PEGDA bioink formulation.

CHAPTER 2

LITERATURE REVIEW

2.1 Introduction to 3D bioprinting

Unlike bones, which have the natural ability to heal over time, the articular cartilage, unfortunately, has a limited capacity for self-repair due to the absence of blood vessels, making treatment efforts a challenge (Cui et al., 2012; Fox et al., 2009). Current treatments used in clinical practice include symptomatic and restoration procedures (Medvedeva et al., 2018; Zylińska et al., 2018). Symptomatic treatments are generally prescribed painkillers and non-steroidal anti-inflammatory drugs (NSAIDs) that offer pain relief while restoration treatments utilise surgical approaches which involve reconstructing the damaged articular cartilage and total joint replacement. However, these treatments require prolonged rehabilitation and complications can arise, such as donor shortage and immunologic response associated with these methods (Medvedeva et al., 2018; Zylińska et al., 2018). There is also the option of synthetic prosthesis for the articular cartilage treatment. However, prosthetic replacement of the articular surface is primarily recommended for patients aged 60 or above who are leading a sedentary lifestyle. Consequently, patients below the age of 45 are not considered ideal candidates for undergoing total knee replacement surgery (Bhosale & Richardson, 2008). This treatment option limits its applicability across age groups and is not deemed suitable for patients who lead an active lifestyle.

The 3D bioprinting technique offers the advantage of a more long-term solution with improved control over the architecture of the 3D construct, allowing the engineered tissue to mimic the native cartilage tissue (McGivern et al., 2021). Structural similarity between the engineered and native tissue will encourage better cell-to-cell communication, consequently increasing the chance of successful

regeneration (Agarwal et al., 2020). The layer by layer deposition of the cell-laden biomaterials follows predetermined movements of the nozzle that is set using a computer aided (CAD) software (Cristóvão, 2018). This motion system facilitates the movement of the bioprinter in x-, y-, and z-axes manner and the deposition of the bioink is controlled by a dispensing system through the bioprinter head (Ozbolat et al., 2017). Using this approach, complex 3D tissue constructs can be designed using the CAD software to customise to fit the patient's specific needs, offering individualized treatment option.

2.2 3D Bioprinting Techniques

Several types of bioprinting techniques that are typically used in the fabrication of 3D constructs for tissue engineering applications are laser-assisted, inkjet and extrusion-based (McGivern et al., 2021). Figure 2.1 presents the schematic diagram of the three main types of bioprinting techniques. The inkjet and extrusion-based bioprinters are one of the most common choices used in 3D bioprinting due to its affordability and wide availability (Kačarević et al., 2018; Mandrycky et al., 2016).

Laser-assisted bioprinters use lasers as an energy source to deposit biomaterials onto a substrate. It consists of three main components; a pulsed laser source, a ribbon coated with a liquid biomaterial and a receiving plate (Li et al., 2016). Laser assisted bioprinters is advantageous for printing high resolution constructs of up to a 10 μm scale, thus, allowing more precise control over the print output (Kačarević et al., 2018). However, laser-assisted bioprinters are less popular compared to other types bioprinters due to its high cost and complex preparation and operating system which consequently limits its scalability (Kačarević et al., 2018; Mandrycky et al., 2016).

Inkjet and extrusion based bioprinters on the other hand are relatively low in cost and more user-friendly, given their simple components and readily accessible design and control software (Soloman, 2020). Inkjet bioprinters involves a drop by drop secretion of the bioink in liquid form through an output nozzle (McGivern et al., 2021). The droplets are ejected by pizelectric or thermal actuation to form the desired pattern and must be solidified before the subsequent layer is deposited to produce a precise complex structure (Wang et al., 2016). Although inkjet bioprinters are cell friendly and support cell viability, the cells can only be printed in low densities as high cell concentration may contribute to nozzle clogging (Mandrycky et al., 2016; Wang et al., 2016). Cui and colleagues reported that a maximum cell concentration of 8×10^6 cells/mL can be used to obtain optimal printing resolution in inkjet bioprinting (Cui et al., 2010). Additionally, the liquid bioink requirement make it difficult for cell encapsulation due to the low viscosity of the bioink (Kačarević et al., 2018; McGivern et al., 2021). Furthermore, the use of low viscosity biomaterial also limits the fabrication of more complex structures that have larger heights especially for cartilage and bone bioprinting applications (Bishop et al., 2017; Wang et al., 2016).

Extrusion-based bioprinters are operated with a mechanical- or pneumatic pressure driven system that focuses on continuous dispensal of biomaterials through a nozzle (Ozbolat et al., 2017). Extrusion based bioprinters have the advantage of bioprinting highly viscous bioinks, allowing the possibility of a more stable large-scale 3D construct to be printed (Tan et al., 2021). Additionally, it is also compatible with high cell densities which is a favourable factor as it is suggested that bioinks containing high concentration of cells helps in tissue formation post printing (Bishop et al., 2017; Wang et al., 2016). The main drawback of extrusion bioprinting is due to the shear stress exerted during printing that may impact the cell viability. However,

the shear stress exerted during the printing process can be controlled by using suitable a bioink with appropriate rheological properties (Kačarević et al., 2018). The shear thinning property of a bioink is essential in extrusion bioprinting as it helps to reduce shear stress as the viscosity of the bioink is lowered during shear force and ease the flow through the nozzle, thus preventing cell damage (Chimene et al., 2018; Morgan et al., 2020). To date, extrusion bioprinting has been applied in a wide range of applications and show promising potential. A study conducted by Chung and colleagues revealed that myoblasts within the alginate-gelatin bioink demonstrated good viability and was not affected by the printing process across all the experimented pressures of extrusion. The authors suggested that the bioink formulation provided a shield to the cells from the shear force exerted at the nozzle tip (Chung et al., 2013). In addition, the bioprinting of cartilage tissue using hyaluronic acid microgel bioink through extrusion bioprinting demonstrated excellent printability and supported the maturation of 3D printed cartilage-like tissue (Song et al., 2022).

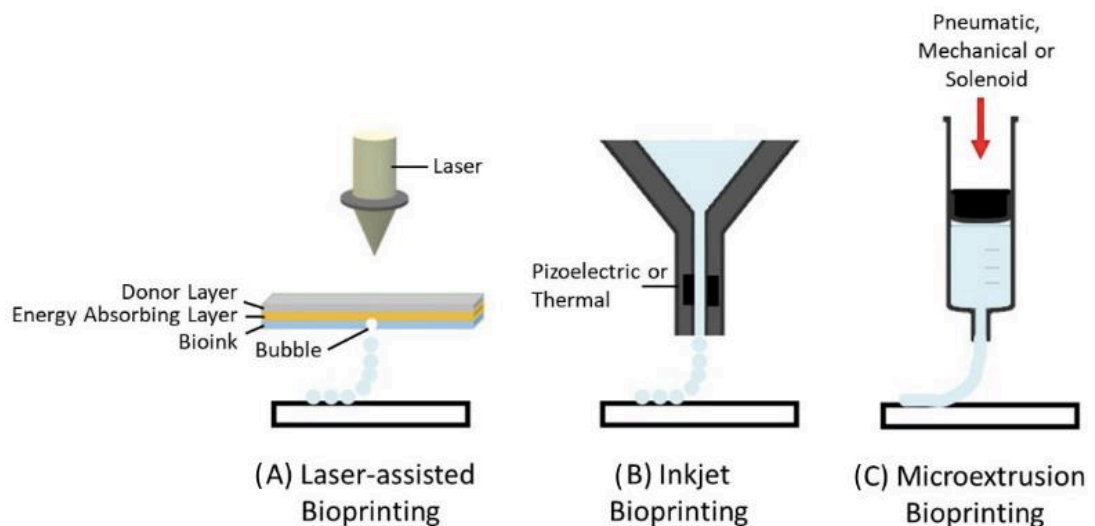


Figure 2.1 Schematic diagram of three main types of bioprinting techniques namely (A) Laser-assisted Bioprinting, (B) Inkjet Bioprinting and (C) Microextrusion Bioprinting. Adapted from McGivern et al., (2021)

2.3 Hydrogel-based bioink for bioprinting applications

Typically, a bioink is made up of hydrogel-based polymers that are chosen based on their desired properties to suit the target tissue type and functionality. Hydrogel based bioink is the gold-standard biomaterials used in tissue engineering applications due to their cross-linking properties and ability to absorb and retain large amounts of water (Ozbolat & Hospodiuk, 2016). The high water content of hydrogels makes them ideal in mimicking the extracellular environment of the native tissues of the human body. The composition of a hydrogel network also allows for permeability of oxygen, nutrients and other water-soluble compounds which is important to encourage uniform cell growth (Teixeira et al., 2022). Hydrogel-based bioinks can be derived from natural or synthetic polymers. Naturally derived bioinks are popularly used in bioprinting applications due to their excellent biocompatibility, low cytotoxicity and biodegradable nature (Tamay & Hasirci, 2021; Teixeira et al., 2022). Some commonly used naturally derived bioinks include alginate, gelatin, collagen and hyaluronic acid.

2.3.1 Alginate

Natural polymers like alginate are one of the most extensively used biomaterial in bioprinting applications due to its intrinsic properties that resembles the environment of the native tissue (Axpe & Oyen, 2016). The high water content and fast gelation property of alginate is highly desirable in extrusion bioprinting as it is able to maintain the viability of encapsulated cells and protect it from shear stress during printing (Datta et al., 2019; Tamay & Hasirci, 2021). Alginate hydrogels are formed through ionic crosslinking in the presence of divalent cations. The sodium ions (Na^+) on the G-blocks of alginate are replaced with divalent cations (Ca^{2+}) to create an egg-box like structure as presented in Figure 2.2 (Abasalizadeh et al., 2020).

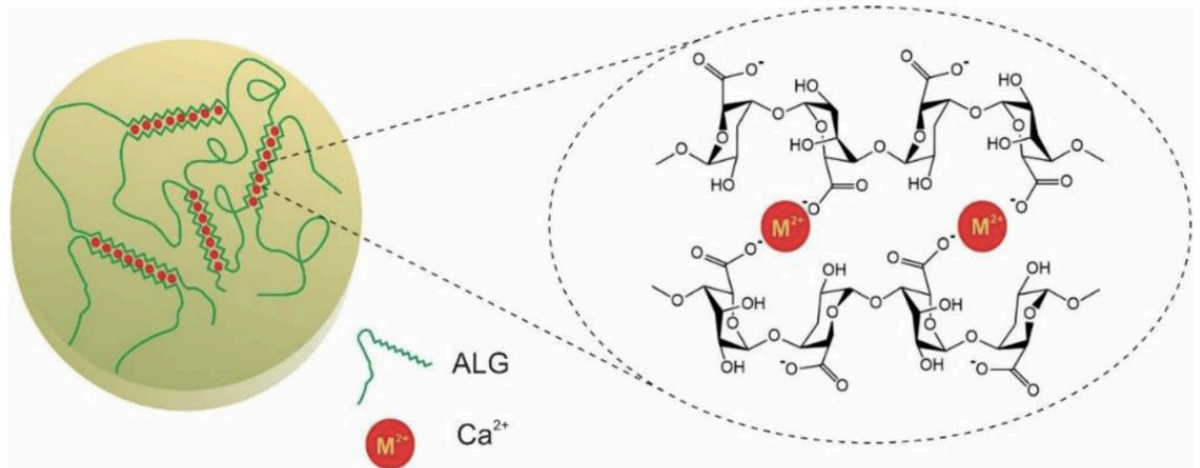


Figure 2.2 Schematic representation of ionic crosslink interaction between alginate and calcium ions forming an egg-box structure. Adapted from Abasalizadeh et al., (2020).

The unique sol/gel state of alginate that allows the conversion between semisolid and solid state is also favourable for extrusion bioprinting. It shows thixotropic behaviour which exhibits low viscosity during extrusion and is later able to regain its stability after extrusion. This is beneficial in retaining its shape during the printing process (Hospodiuk et al., 2017). However, alginate is not suitable to be used just on its own due to several limitations. Some of the major concerns include poor mechanical properties and lack of mammalian cell adhesivity (Li et al., 2018). Although alginate can form ionic crosslinks with cations such as Ca^{2+} to improve its mechanical strength, this physical crosslink is not stable nor long lasting. The reason is because these physical crosslinks are temporary and can be reversed eventually resulting in the disintegration of the hydrogel when incubated in culture medium due to the replacement of divalent cations (Ca^{2+}) by monovalent cations (Na^+) present in the culture medium (Hoffman, 2012). They also lack mechanical stability when printing larger tissue and organ structures (Weng et al., 2021).

Additionally, alginate lack cell binding sites resulting in poor cell attachment and cell proliferation (Gungor-Ozkerim et al., 2018a; Weng et al., 2021). Cell

signaling molecules are crucial for cell adhesion as they determine the growth of new tissues (Hospodiuk et al., 2017). To address these shortcomings, alginate is often combined with other biomaterials to compensate for its limitations. Yang and colleagues found that adding type 1 collagen to alginate-based bioink not only enhanced its mechanical strength but also promoted cell adhesion and proliferation owing to their bioactive properties (Yang et al., 2018). In another study, Säljö and colleagues have also demonstrated that the 3D bioprinted construct printed using a combination of nanocellulose and alginate demonstrated evidence of vascularization and good viability (Säljö et al., 2020). Several studies have also been reported that the addition of nanocellulose as a reinforcement material enhanced the mechanical properties of alginate (Gauss et al., 2021).

2.3.2 Cellulose Nanocrystals (CNCs) as a reinforcing agent

Cellulose is one of the most abundant renewable and sustainable resources in nature. Cellulose are usually obtained from plants but can also be derived from bacteria and algae (Murizan et al., 2020). Nanocellulose is isolated by subjecting the plant or bacteria source to mechanical or chemical treatments (Murizan et al., 2020). The different types of nanocellulose can be divided to nanofibrillated cellulose (CNF), cellulose nanocrystals (CNC) and bacterial nanocellulose (BNC). Owing to its biocompatibility and biodegradability, nanocellulose has been widely studied as a biomaterial in medical applications (Han et al., 2020). Cellulose nanocrystals (CNC) are commonly isolated through acid hydrolysis to produce crystalline rod-like structures (Islam & Rahman, 2018). CNCs have many unique properties such as their high aspect ratio, wide availability and sustainability. These properties are highly desirable in biomedical applications as rheological modifiers and reinforcing agents (Chimene et al., 2020; Gauss et al., 2021).

In addition, the high mechanical strength of nanocellulose have been widely studied to improve the mechanical properties and structural stability of hydrogels (Han et al., 2020). The high surface area, high crystallinity and low elongation at break of CNCs supports the strength of 3D constructs as load-bearing material (Shaheen et al., 2019). According to several studies using alginate based hydrogels for cartilage bioprinting, the high strength and high stiffness of cellulose greatly improved the printability of the bioinks (Han et al., 2017; Markstedt et al., 2015; Müller et al., 2017),. The printed structures not only retained its shape with minimal spreading after extrusion but they also demonstrated improved geometries (Nguyen et al., 2017; Wu et al., 2018).

The high zero shear viscosity and strong shear thinning property also make nanocellulose a desirable materials for extrusion-based bioprinting and improved the printability and low fidelity of the bioink (Ashammakhi et al., 2019; Han et al., 2020). Besides that, the incorporation of nanocellulose also helps in cell adhesion as the nanostructure of cellulose has binding domains and bioactivity that encourages cell response and growth (Hickey & Pelling, 2019). In a study conducted by Shaheen and colleagues, the addition of CNC demonstrated promising cell growth and cell attachment of fibroblasts within the construct. This is contributed by the positive effect CNCs had on the pore structure of the construct which exhibited good interconnectivity and enhanced cell binding, migration and proliferation (Shaheen et al., 2019). Furthermore, La Ferla and colleagues also found that the presence of CNC inhibit bacterial adhesion to human cell lines suggesting that CNCs have antibacterial properties (La Ferla et al., 2018).

2.3.3 Poly(ethylene glycol) diacrylate (PEGDA)

Synthetic polymers have an advantage in mechanical strength which can easily be tuned and modified in order to tailor to the desired requirements (Mao et al., 2020). The combination of both synthetic and natural biomaterials will help to achieve the mechanical and biological properties of the bioink (Gungor-Ozkerim et al., 2018a). PEG has been used with different materials in 3D printing to increase the mechanical properties of the constructs (Gopinathan & Noh, 2018). PEG-based hydrogels are also resistant to non-specific protein adhesion, making them ideal constructs that can promote cell growth and differentiation towards the formation of tissues (Liu et al., 2009). This reduces any immune and inflammatory response within the biological system when the bioink is used as it prevents unwanted interactions with host tissues or cells. Among the PEG-based bioinks, the PEG-diacrylate and methacrylate are widely used polymers in extrusion-based 3D printing (Gopinathan & Noh, 2018).

PEGDA is largely recognized as a successful scaffolding material in tissue engineering because of its biocompatibility and low immunogenicity (Hamid & Lim, 2016). A 3D polymer network is formed by photopolymerization between PEGDA and a photoinitiator such as Irgacure 2959 (Wang et al., 2011). PEGDA consists of double-bond acrylate groups at each end of the PEG chain, giving it the ability to undergo free radical photopolymerization in the presence of the photoinitiator (McAvoy et al., 2018). Figure 2.3 displays the schematic representation of the photopolymerization process of PEGDA and photoinitiator I-2959.

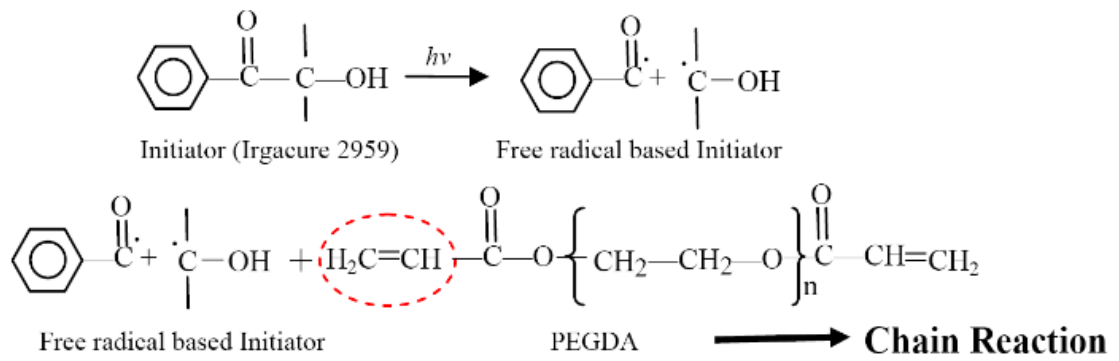


Figure 2.3 Schematic representation of the photopolymerization process of PEGDA and a photoinitiator I2959. The red circled molecule is where the free radical reacts by opening the carbon-carbon double bond. Adapted from Wang et al., (2011).

2.3.4 Double network hydrogel

Double network hydrogel involves a two-step method with a dual crosslinking mechanism. The mechanical dissipation of the double network structure and dynamic sacrificial hydrogen bonds provide the hydrogel with excellent mechanical properties. (Zhou et al., 2020). The primary crosslink typically involves a pregel or partially crosslinked hydrogel that help to maintain the layers during printing while a secondary crosslink contributes to the long-term shape stability of the hydrogel (Schwab et al., 2020). Colossi and colleagues demonstrated the printing of a multi-layered scaffold using alginate-GelMA by relying on two crosslinking mechanism; ionic and UV crosslinking (Colosi et al., 2016). The process firstly involves the gelation of alginate that act as a structural template in maintaining the construct layer during printing when exposed to calcium ions. After the printing process is complete, the construct is then irradiated with UV where GelMA interacts with UV light to form a chemically stable hydrogel. This combination ensures complete bonding between the different layers of the construct and establish the mechanical properties of the printed constructs.

Furthermore, Hong and colleagues have also demonstrated the fabrication of a tough and highly stretchable hydrogel using alginate-PEGDA polymers (Hong et al., 2015). A double network hydrogel with high fracture toughness and promising shape fidelity was achieved by using both ionic and covalent crosslinking via Ca^{2+} and UV irradiation respectively. The reversible crosslinking of Ca^{2+} dissipates mechanical energy under deformation and the long chain of PEG allow for high elasticity and stretchability of the hydrogel. This combination of mechanical energy dissipation and high elasticity results in the formation of a tough yet soft hydrogel. In the bioprinting of hard tissues like the cartilage, high mechanical strength is an important characteristic to consider when formulating a bioink (Wang et al., 2016). The resultant 3D construct needs to be load bearing and possess similar toughness and flexibility as the native articular cartilage (Xu et al., 2013).

2.4 Requirements of a bioink

There are two categories of cell seeding approaches in 3D bioprinting applications. The first approach is a cell-scaffold based approach while the other category is a scaffold-free cell based approach (Gopinathan & Noh, 2018). The cell-scaffold based approach involves a bioink that consists of both the biomaterials and cell suspension, which are then printed to form the desired 3D construct. On the other hand, for the scaffold-free cell-based approach, the live cells are directly printed without any biomaterial. The scaffold functions as structural support for cell attachment and encourage tissue development (Chan & Leong, 2008). To fabricate a successful 3D scaffold, the ideal bioink should satisfy the following requirements; mechanical properties, printability, biocompatibility and shape and structure (Gopinathan & Noh, 2018; Wang et al., 2015).

2.4.1 Mechanical Properties

The mechanical and physical properties of the hydrogel including its internal architecture should match the properties of the native tissue (Semba et al., 2020). The closer the resemblance of the construct properties to the actual tissue environment, the higher the possibility for successful regeneration. Suitable mechanical properties of constructs are very important to provide direct support to the surrounding tissue especially in load-bearing applications (Martínez Ávila et al., 2016).

The mechanical properties of hydrogels are typically assessed by a compression test to determine the compressive modulus of the hydrogel. The compressive modulus of the native articular cartilage ranges from 240 to 1000kPa (Beck et al., 2016). This compression test analysis offers useful insight on the structural mechanical properties of the hydrogel to compare between the formulated hydrogel and the target native tissue. For both natural and synthetically derived hydrogels, the concentration of the biomaterial greatly influences the mechanical strength of the hydrogel. Giuseppe and colleagues reported in their study that an increase in the concentration of alginate-gelatin and duration of crosslinking greatly increased the compressive modulus of the construct. This is due to the increase in the density of alginate and gelatin polymers which influence the strength of the hydrogel (Giuseppe et al., 2018). Similarly, higher PEGDA concentrations results in a hydrogel with much higher compressive modulus and compressive stiffness. However, PEGDA with lower molecular weight resulted in brittle hydrogels (Nguyen et al., 2012). Therefore, in order to obtain the desired mechanical properties of the hydrogel, the concentration, duration of crosslinking period and molecular weight of the polymers need to be optimised to match the properties of the target tissue.

Additionally, the appropriate mechanical properties also serve to provide a proper microenvironment for the cells. It has been suggested that the stiffness of the scaffold and stresses generated from the cell-scaffold strains substantially affect a cell's fate especially for stem cell differentiation (Semba et al., 2020). Therefore viscoelastic behaviour is one of the key parameters to be addressed (Kocen et al., 2017). The swelling behaviour of the hydrogel is also suggested to influence the biomimicry properties of the hydrogel. High water content is favourable as it has close similarity to that of the natural tissue (Bociaga et al., 2019). However, hydrogels with more than 90% water content are very weak and have limited practical applications in tissue engineering (Liu et al., 2018). In short, an ideal bioink should have the right balance between sufficient water content and mechanical strength.

2.4.2 Printability

The hydrogels must be suitable for printer deposition and need to be formulated depending on the requirements of each type of bioprinter. This is because the success rate of printing 3D structures is highly dependent on the printability of the bioink (He et al., 2016). For extrusion-based bioprinting, the bioinks used usually require higher viscosity and shear thinning property (Wang et al., 2015). The printability of the bioink can be fine-tuned by optimising the parameters of a 3D bioprinter. For extrusion bioprinting, the print pressure and print speed are important criteria as they affect cell viability and they can vary from 5×10^{-4} to 400 kPa and 1-30 mm/s respectively (Sánchez et al., 2020). The nozzle gauge diameter which often ranges from 25G to 30G influences the accuracy of the printed structure as smaller diameters gives rise to a higher resolution print (Webb & Doyle, 2017). However, higher gauge or smaller diameter may cause more shear stress on the bioink which can also significantly affect cell viability. This possibility however depends also on the

other print parameters. In a study done by Kang and colleagues using various nozzle diameters, they reported that it did not lead to any significant differences in cell viability (Kang et al., 2013). Therefore, the aforementioned parameters should serve as guidelines during the bioprinting process.

Viscosity is another important factor in the formulation of bioink as it depicts the flow behaviour during printing. Low viscosity tends to contribute to poor printability as it is unable to retain its shape after printing. Higher viscosity bioink on the other hand is more stable and will be able to facilitate the printing of constructs of taller heights (Jose et al., 2016). However, higher viscosity bioink requires higher pressure exerted during printing and may affect the encapsulated cells (Gopinathan & Noh, 2018). Hong and colleagues had pointed out in their research that it is preferable that the pre-gel solution has lower viscosity at high shear rate and higher viscosity at low shear rate (Hong et al., 2015). This is important to ease the flow of the bioink through the extruder of the printer and at the same time to retain the shape of the construct once it is printed. Thus, the printed structure will need to possess adequate stiffness to retain the shape of the 3D structure while also supporting cellular behaviours (Gopinathan & Noh, 2018).

2.4.3 Shape and Structure

It is important for the printed construct to have adequate similarity to the natural tissue in terms of shape and structure (Wang et al., 2015). This is to ensure the printed constructs are able to mimic the actual microenvironment of the native tissues as this factor plays an important role in cellular behaviour (Loh & Choong, 2013). The printed 3D constructs should have interconnected open porosity to facilitate the diffusion of oxygen, nutrients and metabolic waste (Semba et al., 2020). This feature is important in bioprinting and tissue engineering as it enables proper tissue growth

and cell migration as there is good permeability within the construct to the available oxygen and nutrients (Gopinathan & Noh, 2018; Manita et al., 2021). In a study conducted by Gaetani and colleagues, it was observed that the cell viability of the porous cell-laden hydrogel constructs was preserved throughout a 7-day culture. In contrast, the non-porous cell-laden hydrogel constructs showed a significant decrease in cell viability (Gaetani et al., 2012). This is likely due to the factor that cells in a relatively aqueous environment encourage cell migration and matrix deposition as it is not limited by a dense polymer network (You et al., 2017). The 3D construct environment and the internal pore organisation has a direct influence on cell proliferation and differentiation. The porosity of the scaffold affects the growth and regeneration of tissue and organs as they play an important role in nutrient exchange and cell migration. Therefore, the porosity of the bioink should be fine-tuned according to the targeted tissue (Bose et al., 2012; Loh & Choong, 2013).

2.4.4 Biocompatibility

Biocompatibility is an essential requirement of a bioink. Biocompatibility refers to the ability of the biomaterial to perform its desired function without eliciting any undesirable biological effects (You et al., 2017). The bioink should not be toxic, carcinogenic or cause any allergic reaction and adverse immunological response (Tamay & Hasirci, 2021). Generally, naturally and synthetically derived hydrogels that are commonly used in tissue engineering are biocompatible. However, the crosslinking mechanism to form the 3D networks and the printing process may contribute to stress-induced cell damage (Chen et al., 2017; You et al., 2017). Some of the previous studies have reported that calcium concentration of less than 100mM has

the least toxic effect on cells with a more favourable rate of cell proliferation (Bohari et al., 2011; Cao et al., 2012). In addition, the concentration of I-2959 photocrosslinker should be within the range of 0.01% to 0.05% to avoid any significant harm to the cells (Cui et al., 2012; Nguyen et al., 2019). Another important factor is the UV exposure time to the cells which greatly affects the cell viability. The results reported by Nguyen's group found that when the UV exposure time was increased from 1 min to 10 min, the cell viability decreased significantly (Nguyen et al., 2019). This indicate that longer exposure time and higher concentrations of photoinitiator such as I-2959 are presumably cytotoxic towards the cells. Thus, the crosslinking methods should be optimised so that it does not negatively impact the viability of cells. For the printing process, the parameters such as temperature and pressure should also be optimised to favour cell survival in order to minimize any harmful effects to the cell (You et al., 2017).

CHAPTER 3

MATERIALS AND METHODOLOGY

3.1 Materials

The materials retrieved from the manufacturer are graded as analytical grade purity and were applied without further purification.

Table 3.1 List of materials used and the respective manufacturer.

Materials	Manufacturer
Acetic Acid Glacial	QRëC®
Ethanol (99.7 %)	QRëC®
Sulfuric acid (95-97%)	QRëC®
Toluene	QRëC™
Potassium Hydroxide	QRëC®
Sodium chlorite (80 %)	Acros Organics
PEGDA (Mw: 700g/mol)	Sigma Aldrich, Germany
Sodium alginate (MW:216 g/mol)	Sigma Aldrich, Germany
CNC fibres	(manual extraction)
Irgacure 2959	Sigma Aldrich, Germany
Calcium sulphate	Sigma Aldrich, Germany
DMEM basal medium	Gibco, US
Sodium Pyruvate	Gibco, US
Pen-Strep	Gibco, US
Fetal bovine serum (FBS)	Gibco, US
Trypsin-EDTA	Gibco, US
Phosphate Buffer Saline (PBS)	Gibco, US
Trypan blue	Gibco, US

Live/Dead Staining Kit	Invitrogen, US
C2C12 myoblasts	ATCC No. CRL-1772

3.2 Methods

3.2.1 Isolation and Extraction of Cellulose Nanocrystals

The extraction of cellulose nanocrystals (CNC) was adapted using the procedure by Fahma et al., (2010) and Lamaming et al., (2015) with slight modifications. This experiment was conducted at School of Industrial Technology, USM. Firstly, raw oil palm trunk (OPT) fibres obtained from Engcore Agricultural Industries Sdn Bhd were grinded into a smaller size using the Riken grinder with a 1.5 mm filter screen as depicted in Appendix A. The extractives of the fibres were dewaxed for 4 hrs through the Soxhlet extraction method using ethanol/toluene (v/v 2:1) as presented in Appendix B. After drying the extracted fibres at 40°C in the oven, the delignification process was carried out. About 20 g of the sample were bleached in sodium chlorite (NaClO₂) solution under acidic conditions (10% acetic acid solution) at 70°C under agitation of 70 rpm in a water bath incubator shaker for 1 hr and was repeated four times as shown in Appendix C. The bleached fibres were washed with dH₂O until its colour turned white. The hemicelluloses region of the fibres was eliminated by soaking the fibres in 6 wt% potassium hydroxide (KOH) for one day at 4°C as presented in Appendix D. Then, the fibres were washed with dH₂O repeatedly to neutralize the acidic pH of the samples. The samples were subjected to acid-hydrolysis using 210 ml of 64% of sulfuric acid (H₂SO₄) solution under constant stirring at 45°C for 1 hr. Then, 400 ml of cold water was added to the hydrolysed cellulose fibres to terminate the reaction. As presented in Appendix E, the hydrolysed

cellulose was allowed to settle to the bottom of the beaker and the top aqueous layer was carefully discarded and replaced with cold dH₂O. This washing and rinsing step was repeated for at least 15 times until the pH was neutralized. Any residual sulfuric acid was eliminated by subjecting it to dialysis using a dialysis tubing cellulose membrane with a width of 33mm for at least 3 days as depicted in Appendix F. The samples were then homogenised using IKA T-18 homogeniser at 24,000 rpm, sonicated with ULTRASONIK model 28X for 10 mins at low power. Subsequently, the samples were freeze-dried using the Labconco Freeze Dry System with standard settings. The freeze-dried CNC were then grinded into fine powder as shown in Appendix G. The CNC was stored at RT until further use.

3.2.2 Characterisation of the extracted CNC using Transmission Electron Microscopy (TEM)

The characterisation of extracted CNC was carried out using TEM microscopy (EFTEM Libra 120, Carl Zeiss, Germany) at the Electron Microscopy Unit, School of Biological Sciences to determine its size and morphology. A small amount of CNC powder was suspended in distilled water. The CNC suspension was homogenised and sonicated to ensure homogenous dispersion. A drop of the CNC aqueous suspension was placed on a carbon -coated copper grid and allowed to dry. The structure and size of the extracted CNC was then viewed under the TEM.

3.2.3 Preparation of CNC/Alg/PEGDA hydrogel

The selection of the following Alg, CNC, and PEGDA concentrations was based on prior experiments conducted that covered a range of concentrations. Based on the data from prior experiments, the following formulations were prepared based on a two-level experiment with three factors. The two levels chosen were low and high levels that represent the least and most desired concentrations depicted from the

prior data. A center point concentration was also included in this study. These treatment combinations are arranged in an order that introduce the factors one by one with each new factor being combined with the preceding set.

3.2.3(a) Alg solution

The Alg solution was prepared by dissolving sodium alginate powder in dH₂O to make concentrations of 1%, 2.5% and 4% (w/v). The Alg solution was then mixed thoroughly for approximately 1 hr by magnetic stirring under low heat. The mixture was allowed to cool to RT before further action.

3.2.3(b) CNC suspension

Finely ground CNC was weighed and dispersed in dH₂O at concentrations of 2% and 4% (w/v). The CNC suspension was mixed thoroughly using a magnetic stirrer for approximately 1 hr by magnetic stirring at RT.

3.2.3(c) PEGDA solution

The PEGDA solution with molecular weight of 700 g/mol was prepared at 10%, 25% and 40% (v/v) concentrations by the addition of dH₂O at respective volumes. The mixture was stirred at RT for about 30 mins to form a homogenous mixture.

3.2.3(d) Irgacure 2959 solution

The Irgacure 2959 solution was prepared in a dark room by dissolving Irgacure 2959 powder in distilled water to make a concentration of 0.05% (w/v). The solution was dissolved in dH₂O using a magnetic stirrer for about 30 mins at RT until a homogenous mixture is formed. Exposure to light was limited as much as possible.

3.2.3(e) Calcium sulphate suspension

The method of preparation of the calcium sulphate suspension was carried out from the method reported by Freeman et., 2017 with some modifications. The calcium